

## Exceptional transport property in a rolled-up germanium tube

Qinglei Guo, Gang Wang, Da Chen, Gongjin Li, Gaoshan Huang, Miao Zhang, Xi Wang, Yongfeng Mei, and Zengfeng Di

Citation: *Appl. Phys. Lett.* **110**, 112104 (2017); doi: 10.1063/1.4978692

View online: <https://doi.org/10.1063/1.4978692>

View Table of Contents: <http://aip.scitation.org/toc/apl/110/11>

Published by the [American Institute of Physics](#)

---

### Articles you may be interested in

[Raman spectral shift versus strain and composition in GeSn layers with 6%–15% Sn content](#)  
*Applied Physics Letters* **110**, 112101 (2017); 10.1063/1.4978512

[Skyrmion-based high-frequency signal generator](#)  
*Applied Physics Letters* **110**, 112402 (2017); 10.1063/1.4978510

[Uniaxial and tensile strained germanium nanomembranes in rolled-up geometry by polarized Raman scattering spectroscopy](#)  
*AIP Advances* **5**, 037115 (2015); 10.1063/1.4914916

[Realization of direct bonding of single crystal diamond and Si substrates](#)  
*Applied Physics Letters* **110**, 111603 (2017); 10.1063/1.4978666

[Raman-strain relations in highly strained Ge: Uniaxial  \$\langle 100 \rangle\$ ,  \$\langle 110 \rangle\$  and biaxial \(001\) stress](#)  
*Journal of Applied Physics* **121**, 055702 (2017); 10.1063/1.4974202

[Sine-wave gating InGaAs/InP single photon detector with ultralow afterpulse](#)  
*Applied Physics Letters* **110**, 111104 (2017); 10.1063/1.4978599

---



## 5 Electronic Measurement Pitfalls to Avoid

Get the whitepaper

## Exceptional transport property in a rolled-up germanium tube

Qinglei Guo,<sup>1,2</sup> Gang Wang,<sup>3</sup> Da Chen,<sup>3</sup> Gongjin Li,<sup>1</sup> Gaoshan Huang,<sup>1,4</sup> Miao Zhang,<sup>2</sup> Xi Wang,<sup>2</sup> Yongfeng Mei,<sup>1,a)</sup> and Zengfeng Di<sup>1,2,a)</sup>

<sup>1</sup>Department of Materials Science, Fudan University, Shanghai 200433, People's Republic of China

<sup>2</sup>State Key Laboratory of Functional Materials for Informatics, Shanghai Institute of Microsystem and Information Technology, Chinese Academy of Sciences, Shanghai 200050, People's Republic of China

<sup>3</sup>Department of Microelectronic Science and Engineering, Faculty of Science, Ningbo University, Ningbo 315211, Zhejiang, People's Republic of China

<sup>4</sup>State Key Lab of Silicon Materials, Zhejiang University, Hangzhou 310027, Zhejiang, People's Republic of China

(Received 18 January 2017; accepted 4 March 2017; published online 17 March 2017)

Tubular germanium (Ge) resistors are demonstrated by rolling-up thin Ge nanomembranes (NMs, 50 nm in thickness) with electrical contacts. The strain distribution of rolled-up Ge microtubes along the radial direction is investigated and predicted by utilizing micro-Raman scattering spectroscopy with two different excitation lasers. Electrical properties are characterized for both unreleased GeNMs and released/rolled-up Ge microtubes. The conductivities of GeNMs significantly decrease after rolling-up into tubular structures, which can be attributed to surface charging states on the conductance, band bending, and piezo-resistance effect. When illuminated with a light source, facilitated by the suppressed dark current of rolled-up Ge tubes, the corresponding signal-to-noise ratio can be dramatically enhanced compared with that of planar GeNMs. *Published by AIP Publishing.* [<http://dx.doi.org/10.1063/1.4978692>]

Advanced concepts in inorganic semiconductor nano-membrane (NM) science and technology lead foundations for emerging classes of three-dimensional tubular nano/micro-architectonics.<sup>1–3</sup> These tubular architectures, realized by a rolled-up technique, are of interest due to their widely innovative applications in energy storage,<sup>4</sup> robotics,<sup>5,6</sup> electronics/phonics,<sup>7–12</sup> and optoelectronics.<sup>13</sup> With elaborate designs of geometry or surface chemistry during the rolling up process, the corresponding physical properties and device performances can be artificially tuned. For instance, tubular infrared photodetectors are built up by rolled-up III–V NMs, with broadband enhancements in coupling efficiencies, which can be also tuned by the winding numbers of tubes.<sup>13</sup> Photo/electro-luminescence devices have been demonstrated in rolled-up III–V micro-tubes, wherein the corresponding performances can be further tuned by the geometrics of tubes.<sup>14,15</sup> Tubular Si/SiGe heterojunctions are revealed by the rolled-up technique, with the conductivity properties strongly determined by surface charge-trapping states after the rolling process.<sup>9,16</sup>

Nevertheless, germanium (Ge) NM based three dimensional nano/micro-architectonics realized by a rolled-up technique are rarely involved. The rolled-up technique can introduce uniaxial tensile strain in Ge tubes,<sup>17</sup> which may provide a convenient approach for strain-engineering of Ge nanomembrane structures, and thus could lead to infrared light emission.<sup>18</sup> Additionally, GeNMs are considered as promising materials for flexible photodetectors due to their superior mechanical properties and large absorption coefficient.<sup>19,20</sup> Therefore, investigations of electronic or optoelectronic properties of GeNMs under extremely bending

conditions are crucial.<sup>21,22</sup> However, compressing the devices to a radius less than 100  $\mu\text{m}$  by externally mechanical bending remains a major challenge.<sup>8</sup> Shaping GeNMs into three dimensional nano/micro-architectonics with curved profiles by the rolled-up technique would offer ideal platforms for investigating their electronic or optoelectronic properties under severely bending conditions, as the radius of rolled-up GeNMs can easily reach to about 10  $\mu\text{m}$ .<sup>17</sup> Besides, Ge nanomaterials are proved to be extremely susceptible to strain/stress and surface chemistry,<sup>23,24</sup> and constructing GeNM based three dimensional tubular devices and understanding corresponding properties would play crucial roles for their potential applications.

Motivated by these considerations, we focus on single-crystalline GeNM based tubular resistors by the rolled-up approach, and the corresponding electrical properties are revealed in detail. A dramatic decrease in conductivity of a rolled-up Ge tube is observed compared with that of planar GeNM, which is attributed to the surface depletion, band bending, and piezo-resistance effect. In order to estimate the piezo-resistance effect, strain distribution of the rolled-up Ge tube along the radial direction is probed and investigated by Raman spectroscopy with two different excitation lasers. Current-voltage (I–V) characteristics of rolled-up Ge tubes and planar NMs (for comparison) are recorded by utilizing a semiconductor parameter analyzer (Keithley 4200) at room temperature. Furthermore, the optoelectronic response properties are studied with an irradiation laser (405 nm in wavelength), which indicates that the decrease in conductivity is facilitated to reduce the dark current, thus improving the signal-to-noise ratio of GeNM based tubular photodetectors.

Fabrication of rolled-up Ge tubes and tubular resistors is started with a cleaned (100) Ge-on-insulator (GOI) wafer (purchased from IQE Silicon Compounds Ltd.), which

<sup>a)</sup>Authors to whom correspondence should be addressed. Electronic addresses: yfm@fudan.edu.cn and zfdi@mail.sim.ac.cn.

consists of 50 nm top GeNM (phosphorus-doped with a doping concentration of about  $5 \times 10^{17} \text{ cm}^{-3}$ ), 200 nm buried  $\text{SiO}_2$  layer, and silicon substrate. Photolithography and reactive ion etching are utilized to pattern the top GeNM into isolated island array. In order to achieve tubular structures, long-sides of the pre-designed rectangular area for rolled-up tubes (dashed rectangle in Fig. 1(c)) are defined to be parallel to the  $\langle 100 \rangle$  direction of the top Ge layer because the self-rolling direction of single-crystalline semiconductor nano-materials is mainly determined by the Young's modulus.<sup>17,25</sup> Then, second photolithography process is used to define the electrode areas and channel of the tubular device. A stressor layer of chromium (Cr, 20 nm in thickness) is deposited by an e-beam evaporation system to form the initially stressed hybrid Cr/Ge layers. Notably, this Cr layer serves as the stressor layer for the rolling-up process, as well as the electrodes of the tubular resistors. After lift-off, planar GeNM based resistors are constructed, with the channel size of  $2 \mu\text{m} \times 20 \mu\text{m}$ , as shown in Figs. 1(a) (sketched) and 1(c) (optical microscopy image). Immersing the obtained sample into a 40% HF solution to selectively remove the sacrificial layer, i.e., silicon oxide layer, and Cr/Ge hybrid layers (dashed rectangle in Fig. 1(c)) would release and detach from the substrate. Driven by the initial tensile stress in the Cr layer, which is introduced during the deposition,<sup>26</sup> Cr/Ge hybrid layers roll up and form into a tubular structure, as sketched in Fig. 1(b). It should be noted that the channel area can also roll up, which is actuated by the two sides of electrode areas even there is no stressor layer stacking on the channel. The typical optical microscopy image of a rolled-up Ge tubular resistor is shown in Fig. 1(d).

Previous studies have proved that strain can be introduced into the curved films due to the bending effect.<sup>27,28</sup> For example, wrinkled/buckled silicon NMs or GaAs nanoribbons with curved profiles are able to induce continuous strain distributed in NMs.<sup>29,30</sup> In our previous work, uniaxial

strain was also demonstrated in rolled-up Ge tubes, wherein the strain values can be tuned by the diameters of the tubes.<sup>17</sup> However, strain distribution along the depth of the tube-wall is barely involved. Since strain/stress plays a crucial role in modulating the electronic properties and band structures of semiconductors,<sup>31,32</sup> strain distribution along the radial direction in a rolled-up tube is significant and essential to understand the performances of tubular devices. In order to analyse the strain distribution in rolled-up Ge tubes, micro-Raman scattering measurements with two excitation lasers are performed. A rolled-up Ge tube array shown in Fig. 2(a) is fabricated under the same condition for constructing tubular devices, and the average diameter is measured to be about  $10.8 \mu\text{m}$ .

It should be noted that the effective detection depth of the Raman system is determined by the wavelength of the excitation laser.<sup>33</sup> As schematically illustrated in Fig. 2(b), for the 532 nm laser, the penetration depth in Ge is calculated to be about 17.3 nm. For the He-Cd laser with the wavelength of 325 nm, however, only 8.7 nm can be penetrated, which is much smaller than the thickness of GeNMs (50 nm) utilized in this work. The excitation laser powers for both two lasers of the utilized Raman system are tuned down to  $50 \mu\text{W}$  to avoid the local heating effect.<sup>17</sup> Typical Raman spectrums of rolled-up Ge tubes obtained with 325 nm and 532 nm lasers are shown in Fig. 2(c). The corresponding Raman shifts of Ge-Ge vibration modes are summarized in Fig. 2(d). A distinct down-shift in Raman shifts detected by the 325 nm laser is observed compared with that measured by the 532 nm laser, with both peak positions lower than those of unreleased GeNMs. We attribute this to the different penetration depths for two excitation lasers, where only surface signals can be detected for the 325 nm laser; thus, more tensile components contribute to the corresponding Raman spectrum.

Since strain in Ge can affect its electronic structure, the differences between Raman peak positions of rolled-up Ge tubes and bulk Ge are able to be used to monitor the strain state in the Ge tube after releasing. Uniaxial strain ( $\epsilon$ ) generated in rolled-up Ge tubes<sup>17</sup> can be expressed as  $\Delta\omega_{\text{bulk}} = -k \times \epsilon$ , where  $\Delta\omega_{\text{bulk}}$  is the difference of the Ge-Ge Raman shifts of released Ge tube and unreleased GeNM, and  $k = 0.646$  represents a proportionality factor for uniaxial-strained Ge.<sup>32</sup> Therefore, strain distribution along the rolled-up direction (i.e.,  $[100]$  crystal orientation) excited by 325 nm and 523 nm lasers is calculated and plotted in Fig. 2(e) (black squares). Considering the strain variation between the inner and outer surfaces of the tube can be approximately assumed as linear,<sup>34</sup> and also according to the bending theory,<sup>27,28</sup> the top and bottom surfaces of a bent sheet are in tension and compression, respectively. Notably, theoretical tensile and compressive strain components are calculated to be about 0.5% at the outer (depth = 0 nm) and  $-0.5\%$  at inner (depth = 50 nm) surfaces, as shown in Fig. 2(e), which are comparable with the predictions by Raman scattering spectroscopy. Slight discrepancies between experimental and theoretical results can be attributed to the local heating effect even the excitation laser power is set down to 0.05 mW with the spot size of  $1 \mu\text{m}$ .

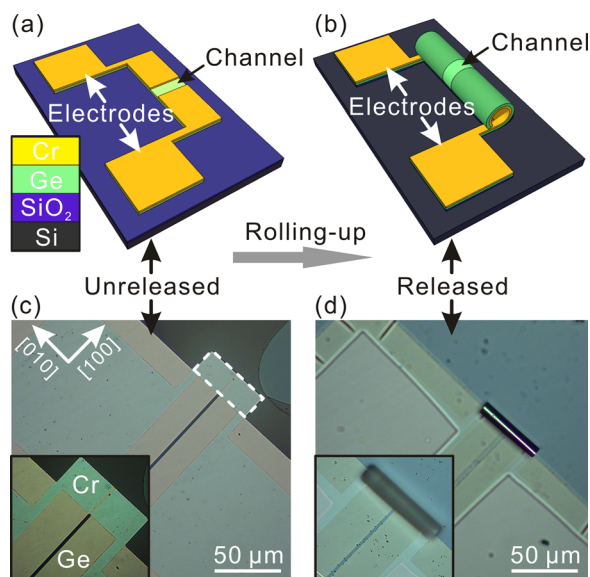


FIG. 1. (a) and (b) Schematic diagrams of GeNM based planar/tubular resistors. (c) and (d) Optical microscopy images of typical planar/tubular resistors. Magnified images show the channel area and chromium electrode areas of GeNM based planar/tubular resistors.

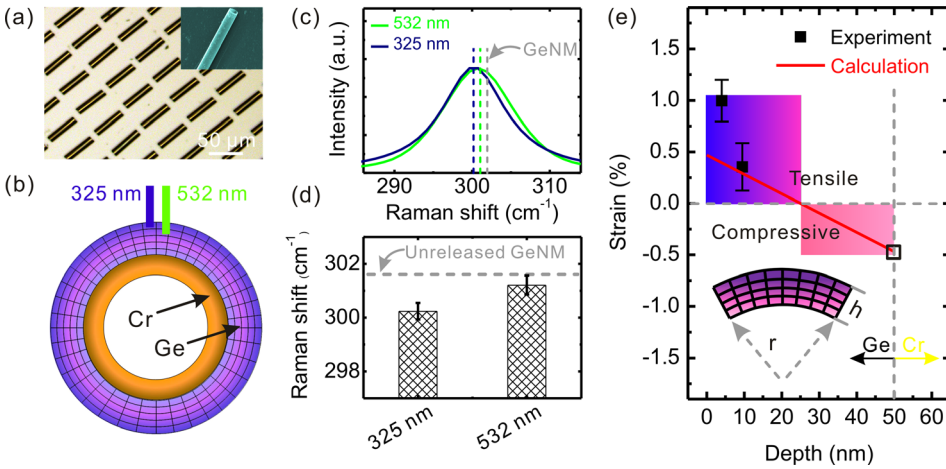


FIG. 2. (a) Optical microscopy image of the released Ge tube array, and a typical Ge microtube observed by the scanning electron microscope is shown in the inset. (b) Schematics of the penetration depth on rolled-up Ge tube excited by two lasers with the wavelengths of 325 nm and 532 nm, respectively. (c) Typical Raman spectra with two excited lasers obtained from the rolled-up Ge tube. The Raman shift of bulk GeNM is highlighted for comparison. (d) Raman shift peak positions with two excitation lasers obtained from the rolled-up Ge tube. (e) Experimental strain distribution and theoretical prediction along the radial direction.

In order to investigate the electrical properties of rolled-up Ge tubular resistors, I–V characteristics are measured. Counterparts of unreleased GeNM based planer resistors are also characterized for comparison. As shown in Fig. 3(a), currents through rolled-up tubular resistors (marked with *Released Tube*) are significantly suppressed compared with those of planar GeNM based resistors (marked with *Unreleased NM*). To verify the electrical transport occurring in the rolled-up tube rather than the Ge/Si junction, which is

formed by collapsed GeNM stacking on the silicon substrate after removal of the sacrificial layer, electrical transport properties of the Ge/Si junction are examined by removing the Ge tube (see the optical microscopy image in the right inset of Fig. 3(a)). The obtained current, shown in the left inset of Fig. 3(a), is more than three orders of magnitude lower than that of Ge tube. Therefore, contributions to the electrical transport of roll-up tubes from the Ge/Si junction can be negligible.

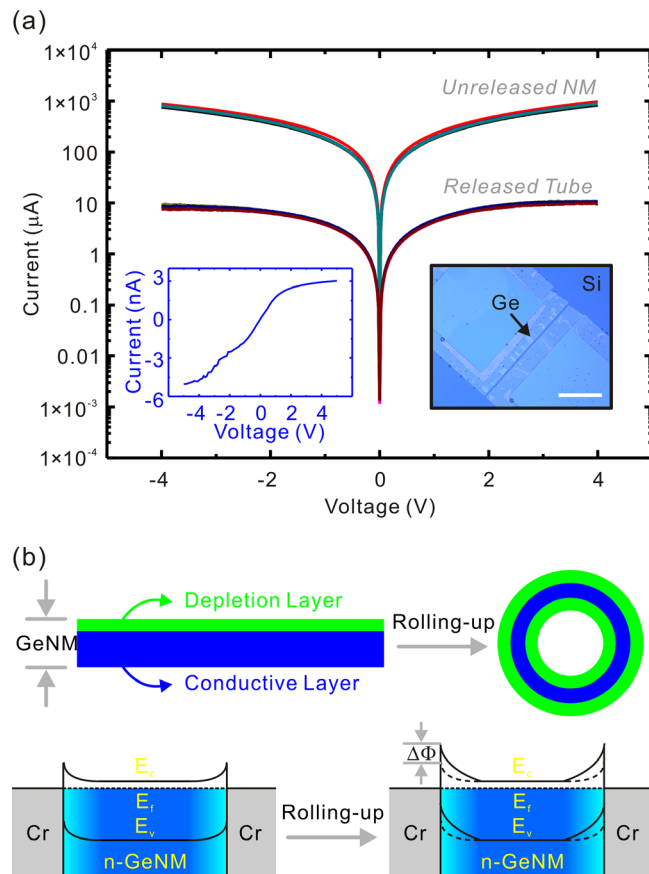


FIG. 3. (a) Current-voltage characteristics of unreleased GeNMs and released Ge tubular resistors. The optical image and electrical property of the collapsed GeNM-Si substrate (Ge/Si) junction after removing the tube are shown in the right and left insets, respectively. Scale bar is 50  $\mu\text{m}$ . (b) Schematic illustration of the depletion layer of GeNM and the rolled-up Ge tube due to charge trapping by surface states. Bottom: Band edge alignment of GeNM resistor and band bending of released Ge tube due to the Fermi level pinning of surface states.

To elucidate the physical mechanism underlying the reduction in conductivity of the Ge tubular resistor, three factors are taken into consideration: (i) surface charging states on the conductance;<sup>9,16</sup> (ii) band bending due to the Fermi level pinning of surface states;<sup>23</sup> and (iii) piezo-resistance effect.<sup>35</sup> A previous study has theoretically pointed out that carrier densities in rolled-up structures could be strongly affected by the surface charged states. Under certain conditions, the channel can even be entirely depleted and becomes nonconductive.<sup>16</sup> Different from unreleased Cr/Ge hybrid layers, a high density of surface states would be generated at both outer and inner surfaces of the tube-wall of the released tubes, which can act as charge traps.<sup>9</sup> Consequently, the effective conducting layer will be shrunken and sandwiched by two depletion layers as schematically illustrated in the top panel of Fig. 3(b), thus leading to decreased conductivity in rolled-up Ge tubes. Additionally, accumulated surface/interface states are proved to be able to induce upward band bending in n-type Ge.<sup>23</sup> Since the high density of surface states can be generated at both inner and outer surfaces of the Ge tube-wall after rolling-up process,<sup>9</sup> the barrier height between Ge and Cr would compliantly increase, as sketched in the bottom panel of Fig. 3(b). Hence, the current flowing through the rolled-up Ge channel could be further decreased.

Except for the above two factors, the piezo-resistance effect in Ge, predicted by Smith,<sup>35</sup> also affects the electrical properties of tubular resistors, wherein compressive strain along the [100] crystal orientation has been demonstrated at the inner surface of rolled-up Ge tubes (see Fig. 2(e)). It should be pointed out that the carrier transport direction, e.g., the channel direction, is along the [010] crystal orientation, as shown in Fig. 1, which is perpendicular to the strain direction, i.e., [100]. Therefore, the change in resistivity ( $\Delta\rho$ ) should be expressed as  $\Delta\rho = X \cdot \rho_0 \cdot \pi_{12}$ , where  $X$  represents the applied stress at the inner surface of the Ge tube,

which is negative for the inner surface of our tubular resistors.  $\pi_{12}$  is the transverse piezo-resistance coefficient in n-type Ge, which is demonstrated to be negative in Ref. 35.  $\rho_0$  is the resistivity under zero stress. Obviously,  $\Delta\rho$  is estimated to be positive, which indicates that the resistivity in Ge tubular resistors is enhanced by compressive strain at the inner surface. In brief, all the above three factors would synergistically contribute to the decrease in conductivity of the Ge tubular resistor. Notably, enhanced surface states after rolling-up are considered to play a dominant role, since they could act as charge traps that deplete the conductive layer and also enhance the barrier height by band bending.

The ability to naturally functionalize rolled-up Ge tubular resistors into state-of-the-art optoelectronic devices represents an essential, defining characteristic of these three-dimensional architectures. The unique advantage can be offered by rolled-up Ge microtubes for the application in photoconductive devices, as the related dark current is distinctly suppressed. I-V characteristics of unreleased GeNM and released Ge tubes under light illumination are explored, as shown in Fig. 4. The light source was provided by a 405 nm laser with the diameter of beam size and light power of about 200  $\mu\text{m}$  and 100 mW, respectively. It can be found that the difference between currents with and without light illumination for the released Ge tube (2.67  $\mu\text{A}$  biased at 2 V) is much smaller than that for unreleased GeNM (72.9  $\mu\text{A}$  biased at 2 V). Under the light illumination, currents increase due to the increment of photon-generated carrier densities. However, for the released Ge tube, more surface states will trap the excited carriers, thus inducing a diminishment in photocurrent. In spite of this, a distinctly enhanced signal-to-noise ratio, defined as the ratio of photocurrent and dark current, can be observed for the rolled-up Ge tube (about 220% biased at 2 V) compared with that of unreleased GeNM (13% biased at 2 V) as shown in Fig. 4, which can be attributed to the significant reduction in dark current.

In summary, GeNMs based tubular resistors are demonstrated by a rolling-up technique. Micro-Raman scattering spectroscopy with two different excitation lasers is performed to investigate the strain distribution in rolled-up Ge microtubes along the radial direction. Exceptional transport properties in rolled-up germanium tubes with significantly decreased conductivities are observed, which can be attributed to surface trapping states, band bending, and piezo-

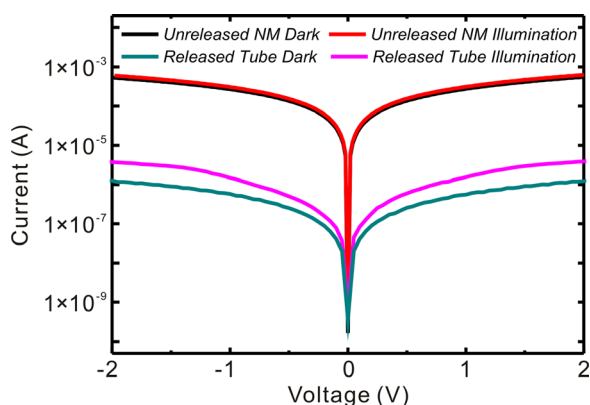


FIG. 4. Current-voltage characteristics of unreleased GeNMs and released Ge tubes with/without light illumination.

resistance effect. The combination of three-dimensional tubular geometry, exceptional electrical properties, and enhanced signal-to-noise ratio under light illumination may render the presented rolled-up Ge microtubes as good candidates for the applications in three-dimensional electronic components, microfluidic sensors, and photodetections.

This work was financially supported by the National Natural Science Foundation of China under Grant Nos. 51602056, 61274136, 51322201, and U1632115), the General Financial Grant from China Postdoctoral Science Foundation (No. 2015M581523), the Open Project of State Key Lab of Silicon Materials (SKL2014-7), the Science and Technology Commission of Shanghai Municipality (No. 14JC1400200), the National Key Technologies R&D Program of China (2015ZX02102-003), the Changjiang Young Scholars Programme of China and the Program of Shanghai Academic/Technology Research Leader (16XD1404200). Q. Guo acknowledges the support under the International Postdoctoral Exchange Fellowship Program by the Office of China Postdoctoral Council. Part of the experimental work was carried out in the Fudan Nanofabrication Laboratory.

- <sup>1</sup>J. A. Rogers, M. G. Lagally, and R. G. Nuzzo, *Nature* **477**, 45 (2011).
- <sup>2</sup>G. Huang and Y. Mei, *Adv. Mater.* **24**, 2517 (2012).
- <sup>3</sup>J. A. Rogers, Y. Huang, O. G. Schmidt, and D. H. Gracias, *MRS Bull.* **41**, 123 (2016).
- <sup>4</sup>C. Yan, W. Xi, W. Si, J. Deng, and O. G. Schmidt, *Adv. Mater.* **25**, 539 (2013).
- <sup>5</sup>Y. Mei, A. A. Solovev, S. Sanchez, and O. G. Schmidt, *Chem. Soc. Rev.* **40**, 2109 (2011).
- <sup>6</sup>A. A. Solovev, W. Xi, D. H. Gracias, S. Harazim, C. Deneke, S. Sanchez, and O. G. Schmidt, *ACS Nano* **6**, 1751 (2012).
- <sup>7</sup>X. Yu, W. Huang, M. Li, T. M. Comberiate, S. Gong, J. E. Schutt-Aine, and X. Li, *Sci. Rep.* **5**, 9661 (2015).
- <sup>8</sup>D. Grimm, C. C. B. Bufon, C. Deneke, P. Atkinson, D. J. Thurmer, F. Schäffel, S. Gorantla, A. Bachmatiuk, and O. G. Schmidt, *Nano Lett.* **13**, 213 (2013).
- <sup>9</sup>F. Cavallo, R. Songmuang, and O. G. Schmidt, *Appl. Phys. Lett.* **93**, 143113 (2008).
- <sup>10</sup>X. Yu, E. Arbabi, L. L. Goddard, X. Li, and X. Chen, *Appl. Phys. Lett.* **107**, 031102 (2015).
- <sup>11</sup>E. J. Smith, Z. Liu, Y. Mei, and O. G. Schmidt, *Appl. Phys. Lett.* **95**, 083104 (2009).
- <sup>12</sup>J. Kerbst, S. Schwaiger, A. Rottler, A. Koitmäe, M. Bröll, J. Ehlermann, A. Stemmann, C. Heyn, D. Heitmann, and S. Mendach, *Appl. Phys. Lett.* **99**, 191905 (2011).
- <sup>13</sup>H. Wang, H. Zhen, S. Li, Y. Jing, G. Huang, Y. Mei, and W. Lu, *Sci. Adv.* **2**, e1600027 (2016).
- <sup>14</sup>I. S. Chun, K. Bassett, A. Challa, and X. Li, *Appl. Phys. Lett.* **96**, 251106 (2010).
- <sup>15</sup>M. H. T. Dastjerdi, M. Djavid, and Z. Mi, *Appl. Phys. Lett.* **106**, 021114 (2015).
- <sup>16</sup>N. V. Demarina and D. A. Grützmacher, *Appl. Phys. Lett.* **98**, 192109 (2011).
- <sup>17</sup>Q. Guo, M. Zhang, Z. Xue, J. Zhang, G. Wang, D. Chen, Z. Mu, G. Huang, Y. Mei, Z. Di, and X. Wang, *AIP Adv.* **5**, 037115 (2015).
- <sup>18</sup>C. Boztug, J. R. Sanchez-Perez, F. Cavallo, M. G. Lagally, and R. Paiella, *ACS Nano* **8**, 3136 (2014).
- <sup>19</sup>M. Kim, J.-H. Seo, Z. Yu, W. Zhou, and Z. Ma, *Appl. Phys. Lett.* **109**, 051105 (2016).
- <sup>20</sup>Q. Guo, Y. Fang, M. Zhang, G. Huang, P. K. Chu, Y. Mei, Z. Di, and X. Wang, *IEEE Trans. Electron Devices* **PP**(99), 1 (2017).
- <sup>21</sup>M. Cho, J.-H. Seo, D.-W. Park, W. Zhou, and Z. Ma, *Appl. Phys. Lett.* **108**, 233505 (2016).
- <sup>22</sup>G. Qin, K. Zuo, J.-H. Seo, Y. Xu, H.-C. Yuan, H. Liu, Z. Huang, J. Ma, and Z. Ma, *Appl. Phys. Lett.* **106**, 043504 (2015).
- <sup>23</sup>D. Wang, Y.-L. Chang, Q. Wang, J. Cao, D. B. Farmer, R. G. Gordon, and H. Dai, *J. Am. Chem. Soc.* **126**, 11602 (2004).
- <sup>24</sup>D. Wang and H. Dai, *Appl. Phys. A* **85**, 217 (2006).

- <sup>25</sup>L. Zhang, E. Ruh, D. Grutzmacher, L. X. Dong, D. J. Bell, B. J. Nelson, and C. Schonberger, *Nano Lett.* **6**, 1311 (2006).
- <sup>26</sup>A. Thorton and W. D. Hoffman, *Thin Solid Films* **171**, 5 (1989).
- <sup>27</sup>Z. Suo, E. Y. Ma, H. Gleskova, and S. Wagner, *Appl. Phys. Lett.* **74**, 1177 (1999).
- <sup>28</sup>M. Grundmann, *Appl. Phys. Lett.* **83**, 2444 (2003).
- <sup>29</sup>Q. Guo, M. Zhang, Z. Xue, L. Ye, G. Wang, G. Huang, Y. Mei, X. Wang, and Z. Di, *Appl. Phys. Lett.* **103**, 264102 (2013).
- <sup>30</sup>Y. Wang, Y. Chen, H. Li, X. Li, H. Chen, H. Su, Y. Lin, Y. Xu, G. Song, and X. Feng, *ACS Nano* **10**, 8199 (2016).
- <sup>31</sup>J. Welsler, J. L. Hoyt, and J. F. Gibbons, *IEEE Electron Device Lett.* **15**, 100 (1994).
- <sup>32</sup>M. J. Suess, R. Geiger, R. A. Minamisawa, G. Schiefler, J. Frigerio, D. Chrastina, G. Isella, R. Spolenak, J. Faist, and H. Sigg, *Nat. Photonics* **7**, 466 (2013).
- <sup>33</sup>J. Takahashi and T. Makino, *J. Appl. Phys.* **63**, 87 (1988).
- <sup>34</sup>A. J. Baca, J.-H. Ahn, Y. Sun, M. A. Meitl, E. Menard, H.-S. Kim, W. M. Choi, D.-H. Kim, Y. Huang, and J. A. Rogers, *Angew. Chem., Int. Ed.* **47**, 5524 (2008).
- <sup>35</sup>C. S. Smith, *Phys. Rev.* **94**, 42 (1954).